Received: 28 March 2018 | Revised: 29 August 2018 | Accepted: 8 October 2018

DOI: 10.4218/etrij.2018-0153

ORIGINAL ARTICLE

WILEY ETRI Journal

Coupling mechanism of a loop-type ground radiation antenna

Zeeshan Zahid[1] | **Hyeongdong Kim**[2]

[1]Department of Electrical Engineering, College of Signals, National University of Sciences and Technology, Islamabad, Pakistan

[2]Department of Electronics and Computer Engineering, Hanyang University, Seoul, Rep. of Korea

Correspondence
Hyeongdong Kim, Department of Electronics and Computer Engineering, Hanyang University, Seoul, Rep. of Korea.
Email: hdkim@hanyang.ac.kr

The coupling mechanism of a loop-type ground radiation antenna is investigated in this paper. We use the equivalent circuit model of the antenna and a full-wave simulation to explain the coupling mechanism of the antenna. We analyze the effects of various antenna parameters on the coupling between the antenna element and the ground plane to examine the conditions for enhancing the coupling. Based on simulations with the equivalent circuit model, full-wave simulations, and measurements, we propose optimal design considerations for the antenna. The findings of this study will aid the design and understanding of loop-type ground radiation antennas for mobile devices.

KEYWORDS
bandwidth, coupling, Q factor

1 | INTRODUCTION

The importance of electrically small antennas has been emphasized by recent advancements in mobile device technology. At smaller sizes, antennas suffer from inherent problems such as small bandwidth, high Q-factor, and low efficiency [1–3]. Therefore, small antennas are often employed to excite the large ground plane of a mobile device, which acts as a low Q structure, to enhance its radiation performance. The coupling between the antenna element and the ground plane is a measure of how effectively the antenna element excites the ground plane for radiation. Among the various types of small antennas available for mobile devices, a loop-type ground radiation antenna (GradiAnt) is a good choice due to its compact geometry and good performance [1,4–7], which is attributed to its strong coupling with the ground plane. The loop-type feed of the antenna is a magnetic coupling structure that can be implemented in various ways [8]. The coupling between the magnetic loop and the ground current modes is maximized if the magnetic loop is located where the maximum current of the ground plane exists. Therefore, the optimum location of the antenna is at the middle of the longer edge of the rectangular ground plane [9–11]. The effect of ground size was discussed in [12] with respect to dual-band operation; however, the study was limited to a few ground configurations.

The effect of including a feeding capacitor and an inductor for wide-band operation was presented in [13]. The near field of the GradiAnt antenna is predominantly magnetic in nature because of its loop-type antenna structure. A significant impedance mismatch occurs as the source frequency deviates from the resonance frequency of the fields; therefore, it is preferable to achieve a wider bandwidth (low Q factor) in the antenna design [14]. The coupling between the antenna element and the ground plane determines the operating bandwidth and efficiency of the GradiAnt antenna [4]; therefore, a comprehensive understanding of the coupling mechanism is imperative. However, the literature does not fully present an explicit investigation of the coupling of the loop-type GradiAnt antenna. A comprehensive study of the coupling mechanism of the GradiAnt antenna must include an analysis of the equivalent circuit model of the antenna along with a full-wave simulation; for instance, the analysis of coupling in the planar inverted F-antenna (PIFA) proposed in [15,16].

Recently, an equivalent circuit model of the antenna was proposed in [17]; however, it merely explained the behavior

of the GradiAnt antenna, and the coupling mechanism of the antenna was not explained. In this study, we comprehensively examine various aspects of the coupling mechanism of the GradiAnt antenna. We analytically investigate the equivalent two-port network of the antenna, and obtain the expressions for its *Z*-parameters and input impedance. We analyze the effects of the lumped component values on the coupling factor, using a Smith chart. It is observed that the coupling between the antenna element and the ground plane is not a function of a single parameter of the antenna geometry or a lumped component; rather, it is controlled by the combination of antenna geometry, lumped components, and ground plane size. For instance, the coupling can be enhanced by increasing the clearance area of the antenna while decreasing the resonance capacitor at a given resonance frequency. In addition, we analyze the effects of various dimensions of the ground size in a full-wave simulator, and thereby propose the conditions to achieve improved coupling. We fabricated a reference design of the loop-type GradiAnt antenna, for which the measured and simulated results were found to be in good agreement. This investigation yields helpful information for the efficient design and understanding of the loop-type GradiAnt antenna for mobile devices.

2 | COUPLING IN THE GRADIANT ANTENNA ELEMENT

The geometry of a typical loop-type GradiAnt antenna (without a ground plane) is shown in Figure 1A. The antenna element consists of two rectangular loops, namely the outer loop and the inner loop. The outer loop is called the resonance loop and is formed by etching a rectangular clearance in the ground plane. The loop contains the resonance capacitor C_r. The resonance frequency of the antenna can be controlled by the area of the outer loop and C_r. The inner loop is called the feeding loop, and it contains the feeding capacitor C_f. The equivalent two-port network of the antenna element is shown in Figure 1B, where each component corresponds to a physical parameter of the antenna element [15]. In the circuit, the components L_F and C_F represent the inductance of the feeding loop and the feeding capacitor, respectively. The inductance of the outer loop and the lumped capacitor are indicated by L_r and C_r, respectively. The values of L_f and L_r are proportional to the areas of the feeding loop and resonating loop, respectively. The series resistance of the resonance loop is indicated by R_r, whereas the series resistance of the feeding loop has been neglected owing to the small size of the loop.

The feeding loop excites the currents in the resonance loop, which in turn excites the ground plane of the device. Therefore, the coupling between the feeding loop and the resonance loop is significant to the operation of the antenna. In order to analyze the coupling, we introduce Port 2 into the equivalent network of the antenna element. The coupling can be analyzed using the normalized input impedance of the two-port network of the antenna, which is given as [18]:

$$Z_{in} = 1 - \frac{(Z_{12})^2}{Z_{11}Z_{22}}, \tag{1}$$

$$Z_{11} = j\left(\omega L_f - \frac{1}{\omega C_f}\right), \tag{2}$$

$$Z_{12} = Z_2 1 = jwL_f, \tag{3}$$

$$Z_{22} = R_r + j\left(\omega(L_f + L_r) - \frac{1}{\omega C_r}\right). \tag{4}$$

The expression Z_{in} is normalized with respect to Z_{11}. The second term in (1) is the coefficient of coupling [19] between the feeding loop and the resonance loop. This factor is maximized if the resonance frequencies of the feeding and resonance loops are equal to the design frequency of the antenna. This important aspect should be considered when determining the dimensions of the loops for efficient design of the antenna.

3 | NETWORK ANALYSIS OF THE ANTENNA EMBEDDED IN THE GROUND PLANE

The geometry of the GradiAnt antenna embedded in the ground plane is shown in Figure 2A. The coupling between the antenna element and the ground plane is determined by the parameters of the antenna element and the geometry of

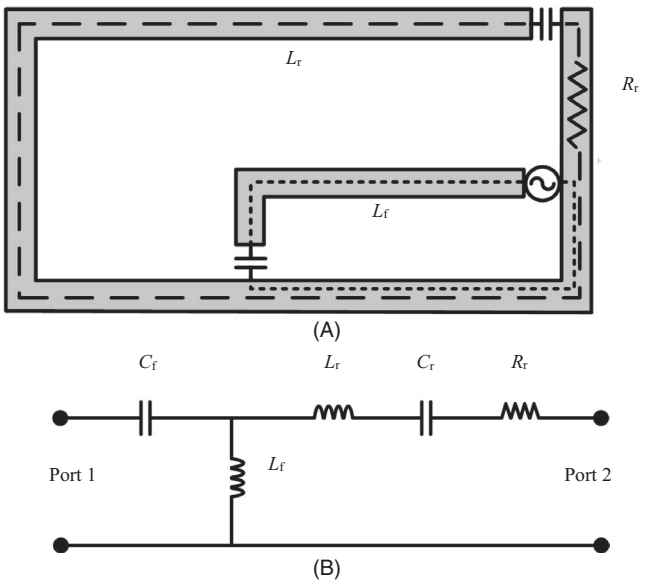

FIGURE 1 Antenna element without a ground plane. (A) The GradiAnt antenna element. (B) Equivalent two-port network of the antenna element

the ground plane. The ground plane acts as a low Q resonator, which can be modeled as a series RLC circuit. Therefore, a series resonator that consists of R_G, L_G, and C_G needs to be added to the circuit model of the antenna element. Figure 2B shows the equivalent circuit of the GradiAnt antenna with the ground plane. It is evident from the network that L_f and C_f constitute an L-type matching network that controls the impedance matching at the design frequency. The circuit can be analyzed using a **Z** matrix, which can be written as:

$$\mathbf{Z}=\begin{bmatrix} j\left(\omega L_f-\frac{1}{\omega C_f}\right) & j\omega L_f \\ j\omega L_f R_T+j\left(\omega(L_T+L_f)-\frac{1}{\omega C_T}\right) & \end{bmatrix}, \tag{5}$$

where L_T, C_T, and R_T represent the total series inductance, capacitance, and resistance, respectively. In (5), Z_{11} represents the impedance of the feed network, while Z_{12} represents the mutual impedance between the feed structure and the ground plane. The expressions of Z_{11} and Z_{12} are given by (2) and (3); however, in this case, Z_{22}, which represents the impedance of both the resonance loop and the ground plane of the antenna, is given by:

$$Z_{22}=R_T+j\left(\omega(L_T+L_f)-\frac{1}{\omega C_T}\right). \tag{6}$$

Using the expressions of Z_{11}, Z_{12}, and Z_{22}, the input impedance of the network can be written as:

$$\begin{aligned} Z_{in}&=Z_{11}-\frac{(Z_{12})^2}{Z_{22}} \\ &=j\left(\omega L_f-\frac{1}{\omega C_f}\right)+\frac{(\omega L_f)^2}{R_T+j(\omega(L_T+L_f)-1/\omega C_T)}. \end{aligned} \tag{7}$$

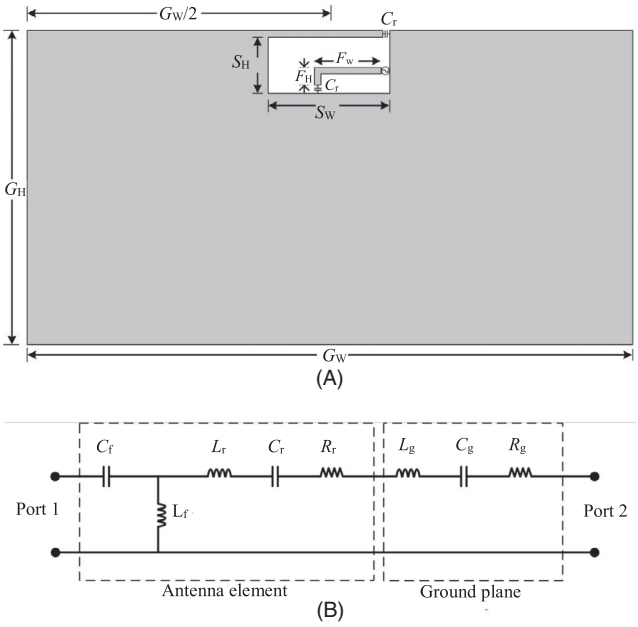

FIGURE 2 Loop-type GradiAnt antenna and its equivalent circuit. (A) Geometry of a typical loop-type GradiAnt antenna embedded in the ground plane. (B) Equivalent two-port circuit model of the antenna

In the expression for Z_{in}, Port 2 has been short-circuited. We use the term Z_c to represent $(Z_{12})^2/Z_{22}$. The resonance frequency of the ground plane cannot be tuned arbitrarily, as it depends on its size. Therefore, the method of coupling enhancement presented in Section 2 is not suitable for the circuit shown in Figure 2B. To analyze the coupling mechanism in this case, we first observe the behavior of Z_{in}, Z_{11}, and Z_c, separately. This is accomplished by modeling the behavior of a GradiAnt antenna operating at 2.45 GHz using the circuit shown in Figure 2B. For this, a reference GradiAnt antenna was designed using the full-wave simulation software HFSS 15. The dimensions of the antenna are presented in Table 1. The values of C_r and C_f are 0.15 pF and 0.55 pF, respectively.

The values of C_r and C_f of the fabricated antenna were 0.21 pF and 0.25 pF, respectively. We used FR-4 ($\varepsilon r = 4.4$, $\tan(\delta) = 0.02$, $h = 1$ mm) as the substrate. Figure 3A shows the simulated current density of the antenna at the operating frequency. In this figure, it can be seen that the loop type currents were excited around the antenna, whereas the dipole type currents were excited on the major area of the ground plane. Figure 3B shows the measured radiation pattern of the antenna. The pattern was measured using a 3-dimensional $6 \times 3 \times 3$ mm^3 CTIA OTA anechoic chamber. The pattern resembles that of a half wave dipole antenna, and the measured peak gain of the antenna was 3.2 dBi. The image of the fabricated antenna prototype is presented in Figure 3C.

In order to obtain the equivalent circuit parameters, the feeding and radiating loops were simulated separately. The parameters L_r, R_r, and L_f were calculated by observing the input impedance of the loops at the design frequency. The loss resistance of the feeding loop is neglected, as it is very small. The ground plane was modeled by a series resonator, and the values of R_g, L_g, and C_g were obtained by tuning the circuit parameters in the Agilent design system (ADS) 2009 in such a way that the reflection coefficient of the circuit replicated that of full-wave simulation [15]. The circuit parameters thus obtained are presented in Table 2.

These values were used to plot Z_{11}, Z_{in}, Z_c, and the return loss of the network. Figure 4 shows the network parameters of a typical GradiAnt antenna. Figure 4A illustrates Z_{11}, Z_c, and Z_{in} on the Smith chart for a frequency range of 1 GHz to 4 GHz. In Figure 4A, the curve representing Z_{11} rotates in the clockwise direction along the circle of zero resistance on the Smith chart.

TABLE 1 Dimensions of simulated GradiAnt in mm

GW	GH	SW	SH	FW	FH
50	25	10	4.5	5.5	1.4

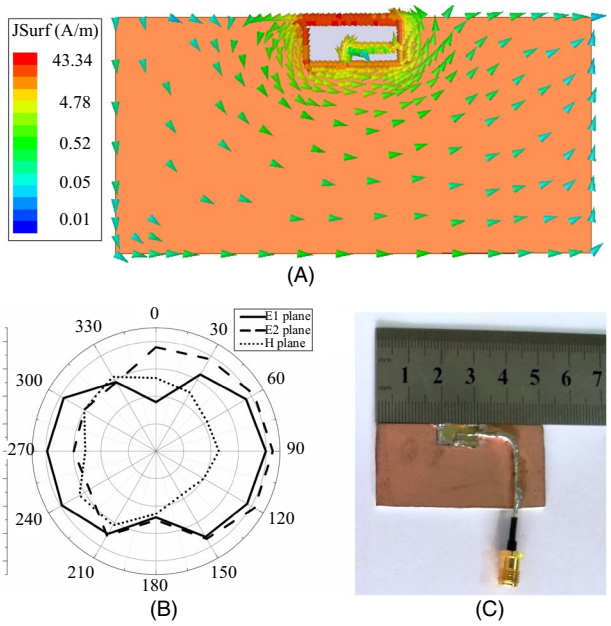

FIGURE 3 (A) Simulated current density and (B) measured radiation pattern of the GradiAnt antenna at 2.45 GHz. (C) Fabricated antenna prototype

The actual starting point of the curve is the open circuit point on the Smith chart, because the feeding capacitor C_f behaves as an open circuit at DC frequency. With increase in frequency, the reactance of C_f decreases while that of L_f increases, and they cancel each other out at resonance frequency. Therefore, the curve of Z_{11} meets the short circuit point on the Smith chart at resonance frequency. The reactance of L_f dominates at frequencies above the resonance frequency, and the curve moves onto the inductive region of the Smith chart. The curve of Z_c starts from the open circuit point on the Smith chart and rotates in the clockwise direction. It passes near the center point of the Smith chart at resonance frequency. The reactance of Z_c at frequencies below the resonance frequency is inductive, whereas that above the resonance frequency is capacitive. This is opposite to the behavior of Z_{11}. At the resonance frequency of Z_{11}, the input impedance is mainly decided by Z_c. A loop is introduced in the curve of Z_{in} by Z_c, which passes near the center of the Smith chart at resonance frequency for a well-matched antenna. The more the points of Z_{in} remain inside the SWR circle of 0.3 (–10 dB reference), the higher the coupling with the ground plane. Figure 4B shows the simulated and measured return losses for a frequency range of 2 GHz to 2.9 GHz. The return loss was measured using a vector network analyzer (Agilent 8753ES). The simulated and measured bandwidths of the antenna were 435 MHz and 460 MHz, respectively. It can be observed that the simulated return loss of the equivalent circuit model and the full-wave simulation fairly overlap. This indicates that the proposed circuit adequately models the behavior of GradiAnt antenna. The measured return loss is also in good agreement with the simulated results.

The coupling between the feeding loop and the ground plane is presented using the circuit model of the antenna. The impedance bandwidth is used as the criterion for determining the strength of the coupling. Figure 5 illustrates the effect of changes in the circuit parameters of Z_{11} on the coupling, for given values of L_T, C_T, and R_T. The values of C_f and L_f were changed inversely, that is, with an increase in the value of L_f, the value of C_f was decreased. The simulations were conducted for the following three cases: (1) L_f = 4.9 nH, C_f = 1.15 pF, (2) L_f = 6.56 nH, C_f = 0.78 pF, and (3) L_f = 8.6 nH, C_f = 0.56 pF. The simulated reflection coefficient is presented in Figure 5A, which shows that increasing L_f while decreasing C_f increases the size of the loop in the curve of Z_{in} and moves it toward the center of the Smith chart, which improves the coupling. The improved coupling results in a larger matching bandwidth. This observation was verified experimentally on the fabricated antenna. The lower value of L_f in Case 1 was implemented by using a smaller feeding loop along with appropriate C_f. Case 2 is that of the reference antenna. A lumped inductor of 6.2 nH was fabricated on the feeding loop of the reference antenna for Case 3. Figure 4B shows the simulated and measured return losses of the equivalent circuit and fabricated antenna, respectively. A good agreement can be observed between the simulated and measured results. The measured bandwidths of Cases 1, 2, and 3 are 50 MHz, 435 MHz, and 660 MHz, respectively. This data shows that the bandwidth of the antenna is the lowest for Case 1 and the highest for Case 3. A further increase in L_f may deteriorate the coupling; therefore, in order to achieve maximum coupling, there is an optimum ratio between L_f and C_f that needs to be employed carefully. This observation can be interpreted as follows. Increasing the area of the feeding loop or using a series inductor in the feeding loop along with an appropriate value of C_f creates stronger coupling with the ground plane. This finding reveals that the feeding loop can be used to improve the coupling and bandwidth of the antenna. This observation is in agreement with an earlier study [13].

TABLE 2 Values of the components of the two-port network of a GradiAnt antenna with a ground plane

C_f (pF)	L_f (nH)	C_r (pF)	L_r (nH)	R_r (Ω)	C_G (pF)	L_G (nH)	R_G (Ω)
0.78	6.56	0.14	28.65	3.14	0.14	29.42	140

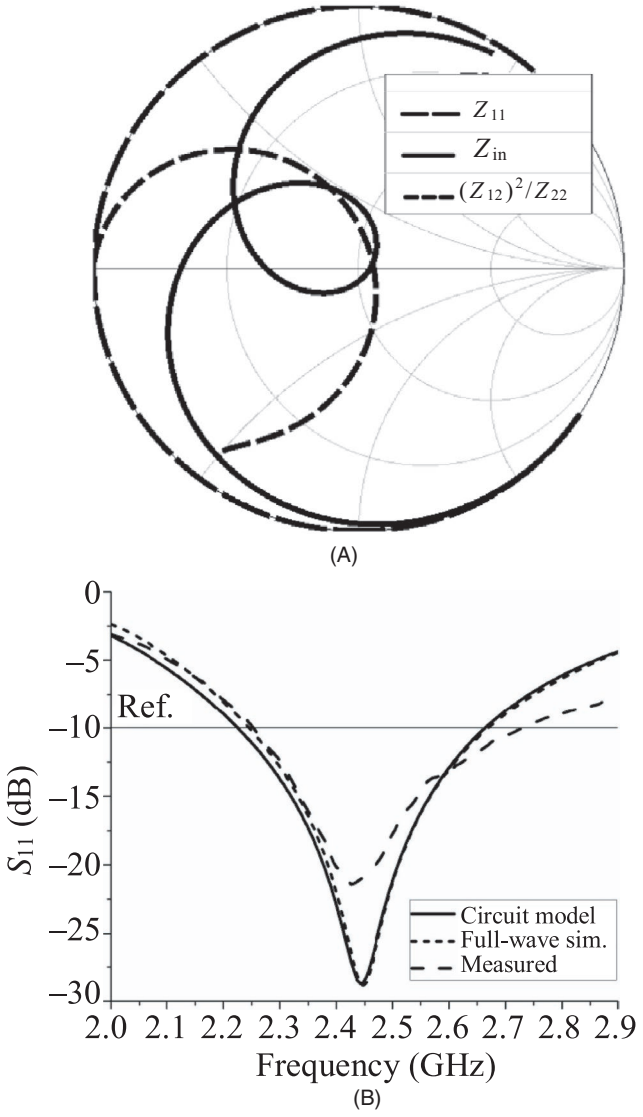

FIGURE 4 Network parameters of a GradiAnt. (A) Plot of Z_{in}, Z_{11}, and Z_c on the smith chart. (B) Simulated and measured return

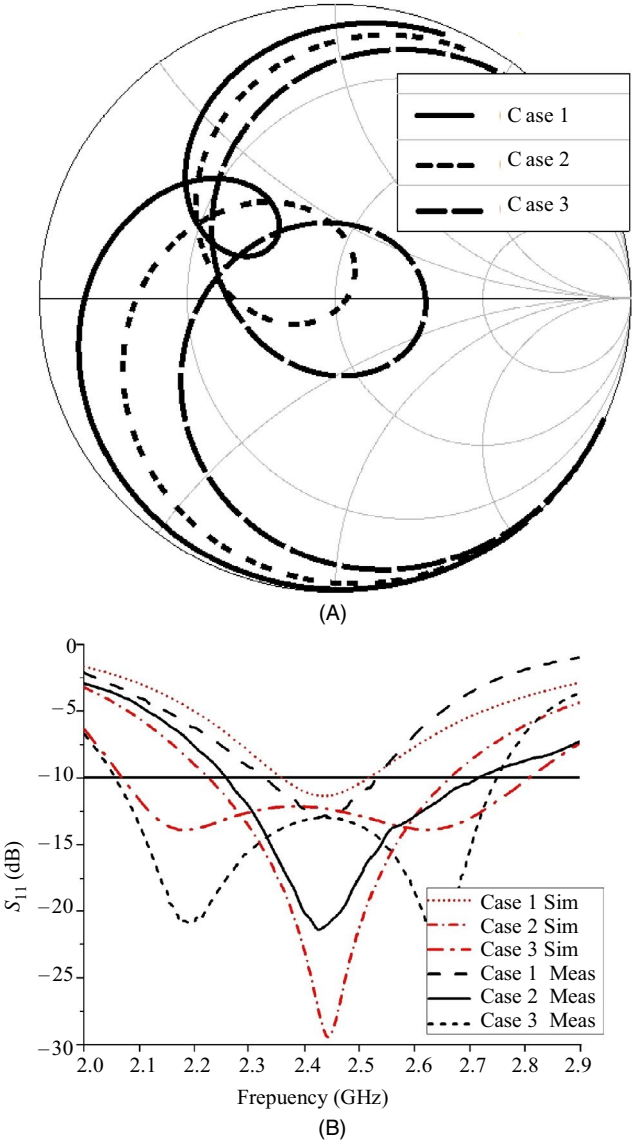

FIGURE 5 Effects of change in Z_{11} for different values of C_f and L_f. (A) Curves of Z_{in} on smith chart. (B) Effect on return loss

4 | COUPLING BETWEEN THE ANTENNA AND THE GROUND PLANE

The size of the antenna is determined by the clearance area etched in the ground plane and is a critical parameter that affects the coupling of the antenna with the ground plane. The parameter L_r of the network shown in Figure 2B models the area of the antenna; however, changing the area of the antenna also affects the ground parameters L_g and C_g. Therefore, a two-port network is not suitable for observing the effect of changes in the clearance area of the antenna on the coupling. The following cases of clearance areas were considered: (a) 8×4 mm^2, (b) 10×5 mm^2, and (c) 12×6 mm^2. The effect was observed using full-wave simulations in which the area of the feeding loop was fixed at 7×2 mm^2. The geometry of the reference design is shown in Figure 2A. It should be noted that in the simulations, conduction and dielectric losses were not taken into account. The parameters C_r and C_f were tuned in order to maintain the resonance frequency and impedance matching. The observations were verified through measurement as well. Figure 6 shows the simulated and measured return losses with the changes in the clearance area. The simulated bandwidth of Cases (a), (b), and (c) were 270 MHz, 435 MHz, and 650 MHz, respectively, whereas the measured bandwidths were 380 MHz, 460 MHz, and 755 MHz, respectively. Again, the measured results are in agreement with the simulated results. This data demonstrate that the bandwidth increases with increase in the clearance area of the antenna. Therefore, the coupling between the antenna

and the ground plane can be enhanced by increasing the size of the antenna.

The size of the ground plane also affects the coupling between the antenna and the ground plane. Observations were made for ground heights of 25 mm, 20 mm, and 15 mm, with the dimensions of the antenna element and the width of the ground plane unchanged. The simulated and measured return losses of the antenna for these ground heights are presented in Figure 7. The simulated bandwidths of the antenna for ground heights of 25 mm, 20 mm, and 15 mm were 435 MHz, 680 MHz, and 740 MHz, respectively. This shows that the coupling increases with decrease in the height of the ground plane. These observations can be explained based on the interactions between the antenna element and the dominant current mode of the ground plane. Figure 8 shows the excited dominant mode on the ground plane. With a decrease in the size of the antenna, the interaction between the antenna and the ground mode increases, resulting in higher coupling. Furthermore, a decrease in the height of the ground plane increases the current density around the antenna, producing the same effect.

The GradiAnt antenna is a magnetic coupler that shows the maximum coupling when it is located at the position of maximum current density on the ground plane. The location of maximum current depends on the width of the ground plane. The current is always zero at the edges of the ground plane; therefore, the coupling of the GradiAnt antenna is at its minimum at that location. If the width is half of the wavelength, as in the case of the reference antenna, the maximum current of the ground mode exists at the middle of the ground; therefore, the middle location is

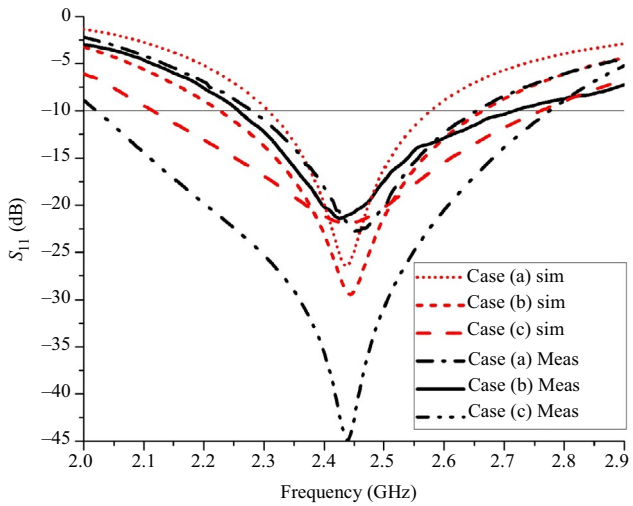

FIGURE 6 Effects of change in clearance area of the antenna

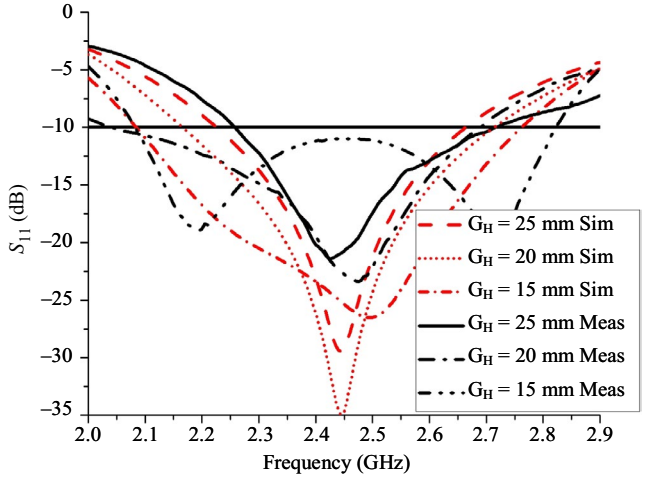

FIGURE 7 Effects of change in ground height

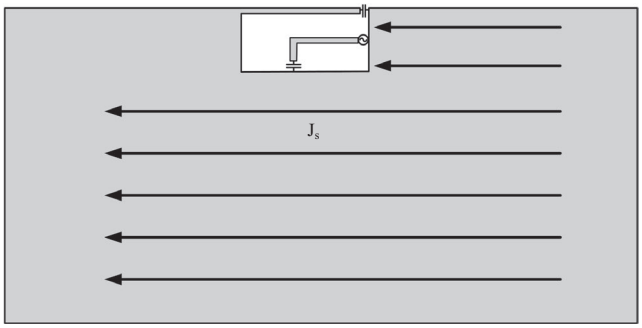

FIGURE 8 Coupling of fundamental ground mode with GradiAnt antenna

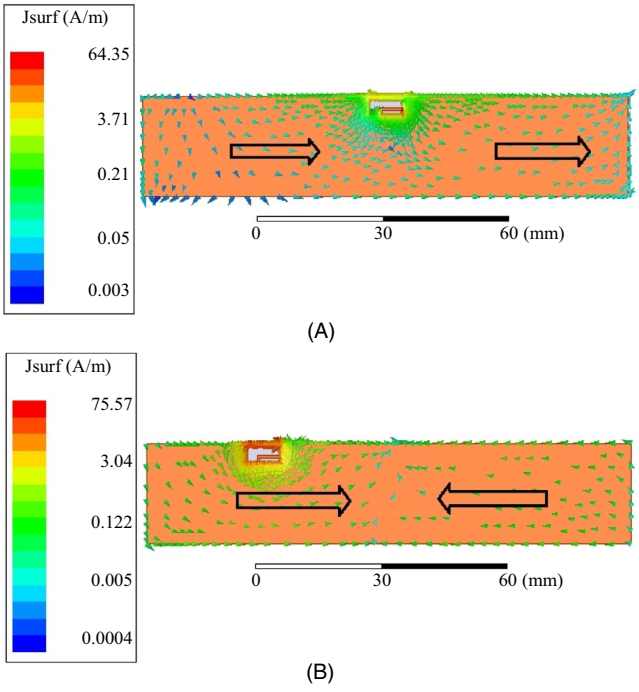

FIGURE 9 Simulated current density of the gradiant antenna at different locations of a 120 × 25 mm^2 ground plane. (A) Middle location. (B) Between the mid and the edge of the ground plane

suitable for the GradiAnt antenna, as shown in Figure 3A. However, if the width of the ground plane is equal to one wavelength, the current density is at its minimum at the middle of the ground plane. Therefore, the middle location is not suitable for antenna placement; rather, it should be located between the mid and the edge of the ground plane. This observation was validated using a ground plane of size 120×25 mm^2. Figure 9 shows the simulated current densities of the antenna at the operating frequency for different locations on the ground plane. Figure 9A shows the simulated current density when the antenna was located at the middle of the ground plane. In this case, the simulated and measured bandwidths were 80 MHz and 85 MHz, respectively, which indicates weaker coupling. Figure 9B shows the current density when the antenna was located 25 mm away from the left edge of the ground plane. The simulated and measured bandwidths of the antenna at that location were 200 MHz and 223 MHz, respectively, indicating stronger coupling. These observations confirm that the antenna must be located at the location of maximum current of the ground mode for stronger coupling.

5 | CONCLUSION

We analyzed the coupling mechanism in a loop-type ground radiation antenna using an equivalent two-port circuit model and a full-wave simulation. Three aspects of coupling were observed between the following: (i) feeding loop and resonating loop, (ii) feeding loop and ground plane, and (iii) antenna clearance and ground plane. We analyzed the conditions for achieving optimum coupling between the feeding loop and resonance loop as well as between the feeding loop and the ground plane by calculating the input impedance of the equivalent two-port network of the antenna. We observed that a higher coupling is achieved if the resonance frequencies of the feeding and resonating loops are close to the operating frequency. A higher L_f and lower C_f also increased the coupling. The equivalent circuit model is more accurate at the design frequency and becomes less accurate when the frequency deviates away from the design frequency; however, the proposed design considerations can be implemented in practical antenna design. In full-wave simulations, we observed that increasing the clearance area of the antenna enhances its coupling with the ground plane. Similarly, decreasing the height of the ground plane also increases the coupling for a given size of the antenna. This discussion is helpful for developing useful insights into the operation and efficient design of a loop-type GradiAnt antenna.

ACKNOWLEDGMENTS

This work was supported by the ICT R&D program of the MSIP/IITP, Republic of Korea (B0101-16-1271, Ground radiation technique for mobile devices).

ORCID

Zeeshan Zahid https://orcid.org/0000-0003-2456-0697

Hyeongdong Kim https://orcid.org/0000-0003-4540-9451

REFERENCES

1. A. H. Wheeler, *Small antennas*, IEEE Trans. Antennas Propag. **23** (1975), 462–469.
2. R. F. Harrington, *Effect of antenna size on gain bandwidth and efficiency*, J. Research **64D** (1960), 1–12.
3. R. E. Collin, *Minimum Q of small antennas*, J. Electromagn. waves Applicat. **12** (1998), 1369–1393.
4. Y. Liu et al., *Loop type ground antenna using resonated loop feeding, intended for mobile devices*, Electron. Lett. **47** (2011), 426–427.
5. O. Cho et al., *Loop type ground antenna using capacitor*, Electron. Lett. **47** (2011), 11–12.
6. H. Choi, Ground radiation antenna, U.S. Patent US8,604,998, 2013.
7. H. Choi et al., Ground radiator using capacitor, U.S. Patent US8,648,763, 2014.
8. Y. Liu et al., *Excitation techniques of loop current mode of ground antenna*, in Proc. Cross Strait Quad-Regional Radio Sci. Wireless Technol. Conf., Harbin, China, 2011, pp. 1732–1735.
9. Y. Liu et al., *Ground radiation using slot with coupling capacitor*, Electron. Lett. **49** (2013), no. 7, 447–448.
10. R. F. Harrington, *Time harmonic electromagnetics*, 2nd ed., Wiley IEEE Press, Hoboken, NJ, USA, 2001.
11. C. A. Balanis, *Antenna theory: Analysis and design*, 3rd ed.,Wiley Inter-science, Hoboken, NJ, USA, 2005.
12. Y. Liu et al., *Loop type ground radiation antenna for dual band WLAN applications*, IEEE Trans. Antennas Propag. **61** (2013), 4819–4823.
13. R. Zhang et al., *Bandwidth enhancement of ground antenna using resonant feeding circuit*, Electron. Lett. **49** (2013), 441–442.
14. M. Salehi et al., *Transient characteristics of small antennas, IEEE Trans*. Antennas Propag. **62** (2014), no. 5, 2418–2429.
15. P. Vainikainen et al., *Resonator-based analysis of the combination of mobile handset antenna and chassis*, IEEE Trans. Antennas Propag. **50** (2002), 1433–1444.
16. J. Lee et al., *Mobile antenna using multi-resonance feed structure for wideband operation*, IEEE Trans. Antennas Propag. **62** (2014), 5851–5855.
17. Z. Zahid et al., *Analysis of ground radiation antenna using equivalent circuit model, IET Microw*., Antennas Propag. **11** (2017), no. 1, 23–28.
18. D. M. Pozar, *Microwave engineering*, 4th ed., John Wiley & Sons, Hoboken, NJ, 2012.
19. C. G. Montgomery et al., Principles of microwave circuits, New ed., Institution of Engineering and Technology, Stevenage, UK, 1986.

AUTHOR BIOGRAPHIES

Zeeshan Zahid received his MS degree in Electronics from Quaid-i-Azam University, Islamabad, Pakistan in 2006. He joined the National University of Sciences and Technology (NUST) as a Lecturer and was promoted to Assistant Professor in 2012. He received the "Best Teacher of the Year" award in 2012. He did his PhD from Hanyang University, South Korea in 2017. Currently, he is serving as the Assistant Professor in the Department of Electrical Engineering, College of Signals, NUST, Rawalpindi campus. His main research interests include high efficiency antenna design for mobile devices, circularly polarized antennas for mobile devices, MIMO antennas, and ultrawide band antennas.

Hyeongdong Kim received his PhD from the University of Texas, Austin, USA, in 1992. He was a postdoctoral fellow at the University of Texas from 1992 to 1993. He is currently a Professor in the Department of Electronics and Computer Engineering, Hanyang University, Rep. of Korea. He has taught various courses such as electromagnetics, microwave engineering, and antenna design, and advanced topics such as MIMO systems that can be used in the 4th generation wireless technology. He specializes in basic and applied research on computational electromagnetics and microwave engineering. His recent research interests include antenna theory and design based on ground characteristic mode analysis, that is, wideband, high-efficiency, circular polarization, MIMO antennas, and high sensitivity antenna.